CANADIAN JOURNAL OF EXPLORATION GEOPHYSICS
VOL. 26, NOS. 1 & 2 (DECEMBER 1990), P. 47-53

MULTIATTRIBUTE PROCESSING OF SEISMIC DATA: APPLICATION TO DIP DISPLAYS

BERND MILKEREIT[1] AND CARL SPENCER[1]

ABSTRACT

We describe two unique aspects of a work station display package used for the interpretation of seismic data. First we introduce new seismic attributes based on the calculation of multitrace seismic coherency estimates, and second we introduce the use of the hue, lightness and saturation (HLS) mixing scheme in the display of seismic images.

Seismic data represent two-dimensional images with amplitude being a function of two coordinates, time and space. Computation of attributes of seismic data introduces new coordinates, resulting in multidimensional images. Most conventional display techniques do not easily accommodate such high data volumes. By using a colour scheme based on hue, lightness and saturation (HLS) up to three seismic attributes can be displayed in a single, composite image. The HLS scheme is best suited to cases where there is a "hierarchical" relationship between attributes in which one attribute is considered of primary importance. In an example, multiattribute processing is applied to simultaneously display and highlight amplitude variations, variably dipping reflections, and coherency variations in a complex seismic data set.

INTRODUCTION

Seismic attributes derived from observed ground motion can assist in the interpretation of the wealth of information present in seismic data. These attributes highlight information additional to that shown in conventional displacement or velocity displays and, when superimposed, are capable of highlighting various structural features in an interpretation. Much progress has been made since displays of frequency content were first used in a colour sonagram process (Balch, 1971); as illustrated in Figure 1, a wide range of attributes can now be assigned to each sample of the observed seismic wave field. They may be grouped into single- or multitrace attributes, based on their method of calculation.

As their name implies, single-trace attributes are extracted from the data one trace at a time. Using techniques such as complex trace analysis or linear inverse theory, estimates of envelope amplitude ($|a|$), instantaneous frequency (ω), phase (θ), polarity (Taner and Sheriff, 1977; Taner et al., 1979) and recovered acoustic impedance (Lindseth, 1979; Oldenburg et al., 1983) may be obtained. Such attributes may be displayed graphically for structural or lithological interpretation of seismic data.

Multitrace attributes are calculated for each sample of the wave field from two-dimensional subsets (or windows) of the input data. For example, coherency estimates can be obtained from semblance or cross-correlation analyses (Milkereit, 1987a; Quincy and Tomich, 1987); slowness, velocity and depth estimates can be obtained from shot or common-midpoint-ordered data by using local slant stacks (Milkereit, 1987b). In addition, there are a number of attributes such as stacking velocities, interval velocities, and variation of Poisson's ratio, which can be obtained from interactive processing of seismic data. For example, Bording et al.

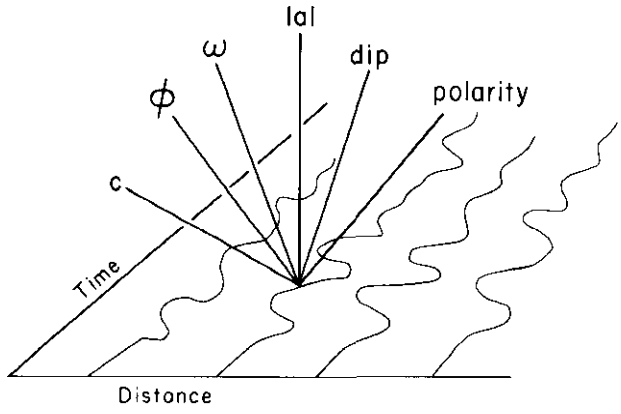

Fig. 1. Attributes of seismic data. Several attributes can be computed and assigned to each sample of the seismic wave field in the time-distance (t-x) domain. Attributes used in this study are amplitude envelope (or reflection strength) ($|a|$), coherency (c) and dip. A multiattribute value $M(x, t)$ is defined as the combination of two or more attributes, and colour coding is used for display purpose.

Manuscript received by the Editor August 18, 1989; revised manuscript received September 1, 1990.

[1]Geological Survey of Canada, 1 Observatory Crescent, Ottawa, Ontario K1A 0Y3

The authors would like to thank L.J. Mayrand, J. Broome and two reviewers for providing helpful suggestions on the manuscript. Geological Survey of Canada contribution 25889 and Lithoprobe publication 196.

(1987) displayed velocities determined by traveltime inversions as an attribute of a migrated depth section.

Once a seismic attribute has been assigned to each sample of a seismic section the attribute data themselves can be considered as a two-dimensional image to which image enhancement or smoothing processes such as median filters, alpha-trimmed means, and illumination (Huang et al., 1979; Horn, 1982; Stewart, 1985; Gersztenkorn and Scales, 1988) may be applied before display. The results of these processes are often displayed as colour overlays to the conventional seismic section allowing correlation with subsurface structure and the easy identification of features such as lateral changes in the wave field.

The use of two or more independent measurements for colour image enhancement is well-known in various geophysical applications such as remote sensing (Watson, 1985), potential field data (Broome, 1989) and gamma-ray spectrometry (Duval, 1983). In general, multiattribute analyses based on colour mixing displays work best with independent, uncorrelated attributes obtained by different attribute extraction techniques. Until recently composite colour displays have found only limited seismic applications. Hardy et al. (1989) described their application to the identification of long-period multiple reflections. Cliet and Dubesset (1987) and Frasier and Winterstein (1990) suggested their use for the polarization analysis of three-component seismic data.

In this paper we propose new interpretational tools, based on combinations of single-trace attributes (such as reflection strength and instantaneous frequency) and multitrace attributes (such as dip and coherency) that are displayed using various mixing techniques. We begin by describing a procedure for automatically estimating the coherency and dip of seismic data. We then discuss some of the practicalities of the multiattribute display of seismic data. Finally, as an example, we show how multiattribute processing can be used to simultaneously display and highlight amplitude variations, variably dipping reflections, and coherency variations in a complex seismic data set.

Dip and coherency attributes of seismic data

Local dip estimates can be obtained from seismic data by manually or automatically tracking horizons and differentiating traveltimes along these horizons (e.g., Dalley et al., 1989). Here we propose the application of an automatic procedure that is based on moving window beam forming (Mikereit, 1987b). The advantage of this approach is that two local attributes, coherency and dip, can be estimated simultaneously for each sample.

Consider a seismic wave field $u(x, t)$ regularly and adequately sampled in both space and time. Let a dip passband be defined for dips p_j, sampled at J equally spaced steps between $p_{\min}$ and $p_{\max}$ so as to include all dips of interest:

$$p_{\min} \le p_j \le p_{\max}, \ (1 \le j \le J).$$

A local coherency estimate $c(x, t)$ may be obtained for each sample of the wave field $u(x, t)$ by moving a limited aperture (L-trace) window across the wave field $u(x, t)$ (e.g., Leven and Roy-Chowdhury, 1984; Milkereit, 1987b; Varsek et al., 1990). Let x_n denote the spatial coordinate of the nth sample of the wave field $u(x, t)$ (Figure 2). For a given dip p_j, the semblance, $s(t, p_j; x_n)$ of the wave field $u(x, t)$ at x_n and at time t is defined as:

$$s(t, p_j; x_n) = \frac{S(t, p_j; x_n)^2}{L \sum_{l=1}^{L} u(x_l, t_l)^2}, \qquad (1)$$

where $S(t, p_j; x_n)$ is the local slant stack (McMechan, 1983) of an L-trace aperture centred at x_n,

$$S(t, p_j; x_n) = \sum_{l=1}^{L} u(x_l, t_l), \qquad (2)$$

and where $u(x_l, t_l)$ is the seismic data at distance x_l and at time

$$t_l = t + p_j (x_l - x_n).$$

The calculation of S involves a series of shift and sum operations and is easily vectorizable. With regularly spaced data the time shifts required do not vary along the line and need to be calculated only once.

For each sample of the seismic section we obtain J coherency measures $s(t, p_j; x)$, each of which has a value between 0 and 1. The lower bound corresponds to complete incoherency and the upper bound to identical amplitudes $u(x, t)$ on all L traces of the aperture. We define a local coherency estimate $c(x, t)$ as the peak semblance value,

$$c(x, t) = \max[s(t, p_j; x)], \ (1 \le j \le J),$$

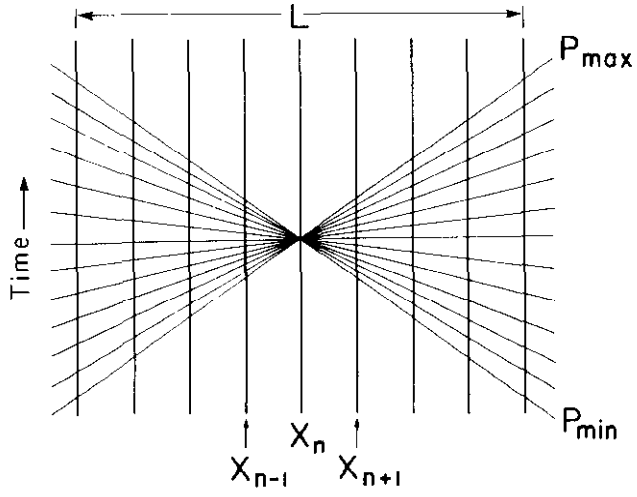

Fig. 2. Beam-forming diagram for multitrace dip and coherency analysis. Maximum and minimum dips are labelled $p_{\max}$ and $p_{\min}$, respectively. x_n is the centre trace of an L-trace wide aperture. The dimensions of dip are given in either s km^{-1} or ms/trace.

and the local dip estimate $p(x, t)$ is defined as the slowness p_j associated with this local coherency estimate*.

The finite aperture slant stacks [equation (2)] and semblance measurements [equation (1)] must be evaluated for each sample of the observed wave field $u(x, t)$. The choice of the number of traces (L) for the finite aperture depends on the lateral extent over which the signal is expected to be coherent. In this paper, we used a 9-trace aperture ($L = 9$) to compute the coherency estimates $c(x, t)$. Tests using noisy synthetic data and a 9-trace aperture demonstrate that local slant stacks provide stable results even for data with signal-to-noise ratios as low as 0.5 (for examples see Milkereit, 1987a, b). The number of beam-forming operations (J) is dependent on the frequency content, spatial-sampling interval and maximum dip of the data, together with computational constraints. Here, we apply 61 beam-forming operations ($J = 61$) covering the user-specified dip passband. Milkereit and Spencer (1990) described a semblance-based filter in the t-x domain to enhance coherent seismic energy by suppressing incoherent background noise that is based on multitrace attributes defined by equation (1).

THE DISPLAY OF SEISMIC ATTRIBUTE DATA

Seismic data are most commonly displayed as monochrome variable area plots. These are ideal for data sets in which the most important information to be displayed is the correlation of events from trace to trace. However, the magnitude of any quantity is often obscured and these plots are of limited use in displaying any other data attributes. Variable density plots and colour variable area plots offer much more flexibility in displaying single-attribute and multiattribute data.

Single-attribute displays

In principle, variable density plots showing a single attribute can use a monochrome grey scale or a colour scale covering a range of hues. In practice, it can be very difficult to produce successful grey scales, and colour manipulation is a much more useful tool. The most important step in creating a colour display is the choice of the function that maps an attribute value into a colour (hue) for display. Let the hue assigned to a particular attribute value a be denoted as $h(a)$. Then one of the simplest mapping functions is,

$$h(a) = \begin{cases} h_{\text{back}} & \text{if } a < a_0; \\ h_0 + \frac{h_{\max} - h_0}{a_{\max} - a_0}(a - a_0) & \text{if } a_0 \le a \le a_{\max}; \\ h_{\max} & \text{if } a > a_{\max}. \end{cases}$$

Here a_0 and $a_{\max}$ represent a low and high cutoff value, respectively, for displaying the attribute. Any value below a_0 is treated as noise and given the background colour h_{back}, whilst values between a_0 and $a_{\max}$ map linearly to the range of hues h_0 to $h_{\max}$. Such a function requires the specification of the five quantities a_0, $a_{\max}$, h_{back}, h_0 and $h_{\max}$. On a work station it is usually possible to support the almost instantaneous modification of the values h_{back}, h_0 and $h_{\max}$ since they involve only the manipulation of palette entries. In some cases, modifying in a_0 and $a_{\max}$ requires a lengthy data rescaling step. However, on machines that support a large number of colours simultaneously rescaling may be simulated by contracting or expanding the colour palette to cover various data ranges. Several more sophisticated palette assignments are commonly used in image processing applications and can be useful in geophysical interpretation. It is quite common to assign colours to data values based on a histogram equalization algorithm which ensures that all colours are equally represented in a display. A more flexible approach (histogram specification) is to interactively group together parts of the palette and assign a single hue to this group. This allows the interpreter to emphasize differences between various ranges of values in the display.

Multiattribute displays

Let several seismic attributes ($a_1, a_2, \ldots, a_n$) be assigned to each sample of the wave field $u(x, t)$. Multiattribute displays of seismic data are used to highlight basic information related to various aspects of the structural or lithological interpretation of the data. The simultaneous display of two or more attributes as a colour display produces a single image to assist in the interpretation of seismic data. Such an image is based on a multiattribute value $M(x, t)$ that is a function of several attributes, e.g.,

$$M(x, t) = f[a_1(x, t), a_2(x, t), a_3(x, t)]$$

for the three-attribute case.

The most important factor in creating a useful multiattribute image is that of the choice of a colour mixing scheme that clarifies the relationship between various attributes and their importance in terms of structural or lithological interpretations. Previous attempts at mixing attributes seem to have been confined to displays in which various intensities of red, green and blue are mixed (the RGB scheme as shown in Figure 3a). It is an excellent method for the display of three independent parameters and where the features to be examined can be expected to produce large areas of uniform colour. However, seismic attributes rarely meet these criteria. Another drawback of the RGB scheme is that it is less suitable for the display of only two attributes because such displays make use of only a limited colour range. For instance, any slice through the colour cube shown in Figure 3a could be used as the palette for a two-attribute mixing scheme. However, none shows the contrasts produced by the hue and lightness display. Finally, care must be taken when producing hard copy from RGB schemes. Composite colour images which show great luminence on a work station screen lose it when they are dumped to paper hard copy devices. An alternative method

*In practice, singularities at zero crossings can be avoided by either performing the slant stack, [equation (1)] over a time window equal to the wavelet period or by applying a median filter to $c(x, t)$ (Milkereit, 1987b; Figure 4).

is to mix attributes in a subtractive scheme (CMY) in which areas to be highlighted appear dark on the paper.

These are only two of a number of possible colour mixing schemes. They have gained popularity because they are used internally by many display devices, but we have found that in many cases hue, lightness and saturation (HLS) schemes produce better results**. The HLS scheme works by describing all possible colours in terms of three quantities. Hue represents the shade of a colour; it is normally expressed as an angle on a circular scale with red as 0 degrees, through yellow, green and blue to violet as 360 degrees. The hue scale is continuous in the sense that each colour can be obtained by mixing its neighbours. Lightness quantifies the overall brightness of a colour with a value of 0 corresponding to black. Finally, saturation quantifies the mixing of a colour having a particular hue and lightness with a grey at the same lightness. Saturations of 0 percent and 100 percent represent pure grey and pure colour, respectively.

We have found that for mixing two attributes the best method is to use hue and lightness. These are two "axes" of the hue, lightness and saturation (HLS) scheme shown in Figure 3b. The scheme is particularly suitable for mixing cases where one attribute represents a quantity important for seismic interpretation, such as apparent dip, and one represents the "quality" of the section, such as amplitude envelope or peak semblance. The first of these attributes is mapped to hue in a similar fashion to that for the single attribute case discussed above, the second is mapped to lightness. In the case of dip and envelope, this will produce a section showing the dip of event emphasized according to the trace amplitude. Careful interactive choice of thresholds is necessary for the technique to be useful. One particularly useful feature of two-attribute displays is the ability to emulate multitrace filtering using the display alone. This is accomplished by interactively setting areas of the palette to the background value so that the display no longer shows the dips or frequencies represented by these colour values.

The natural extension of this scheme to three attributes is to use saturation to represent the third quantity. This can work if the third attribute also represents some measure of data quality, since low saturations reduce the apparent differences between the hues. However, it has its limitations because it is often difficult for the eye to separate the effects of lightness and saturation. The HLS scheme is best suited to cases where there is a "hierarchical" relationship between attributes in which one attribute is considered of primary importance. We will illustrate the HLS scheme displays for a three-attribute image based on dip, amplitude and coherency estimates.

An application of multiattribute displays

An example of the application of multiattribute composite colour images to a real data set is shown in Figures 4 and 5. Figure 4 is a conventional display of a 35-km migrated section recorded as part of a marine seismic reconnaissance survey across the Midcontinent Rift in Lake Superior. A detailed interpretation of the data may be found in Cannon et al. (1989). A relatively thin, almost flat-lying, sequence of strong, continuous reflections from volcanic layering extending from 2 to 3 s two-way time (B in Figure 4) lies unconformably on a synformal structure of Early Proterozoic age (C in Figure 4) consisting of a series

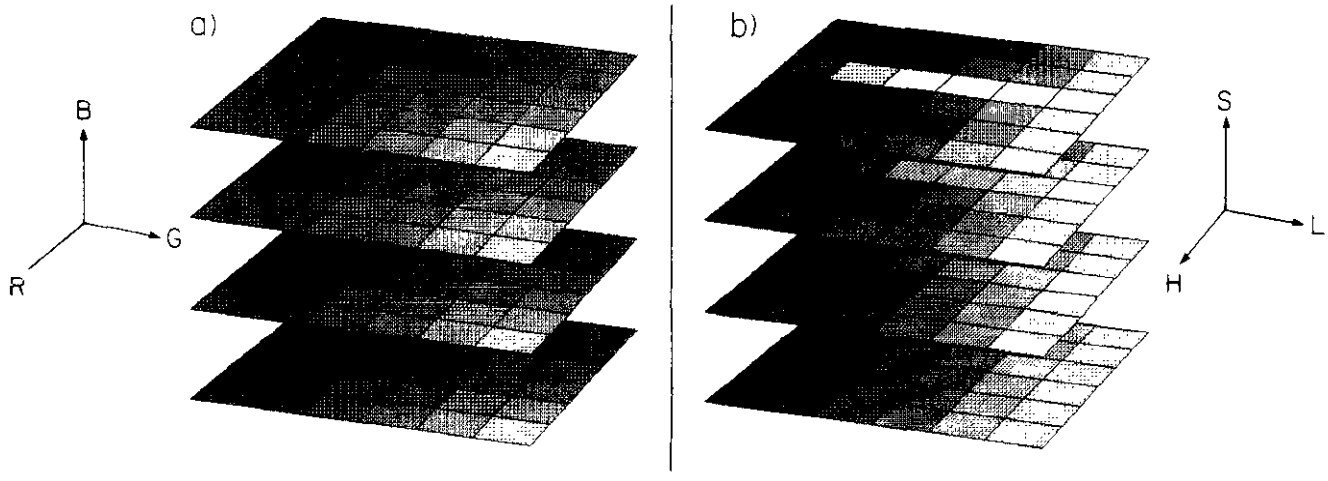

Fig. 3. Examples of multiattribute colour coding. Variations in the multiattribute *M* can be highlighted by defining its colour as a function of **(a)** red, green and blue (RGB) or **(b)** hue, lightness and saturation (HLS).

**Some of the problems associated with RGB and HLS schemes for image processing are discussed by Rots (1989).

of half grabens. The volcanic sequence is overlain by a postvolcanic sedimentary unit (A in Figure 4). The particular problem at hand is that the migrated section shows: (a) several dip directions that are associated with the volcanic sequence and underlying structures of the Midcontinent Rift; (b) lateral dip variations; (c) amplitude variations; and (d) variations in data quality. Of key importance in interpreting the data are the local attributes: reflection strength (i.e., the amplitude envelope), dip directions and coherency.

We used the amplitude envelope calculated using complex trace analysis, together with the dip and coherency estimates calculated using the method described in the

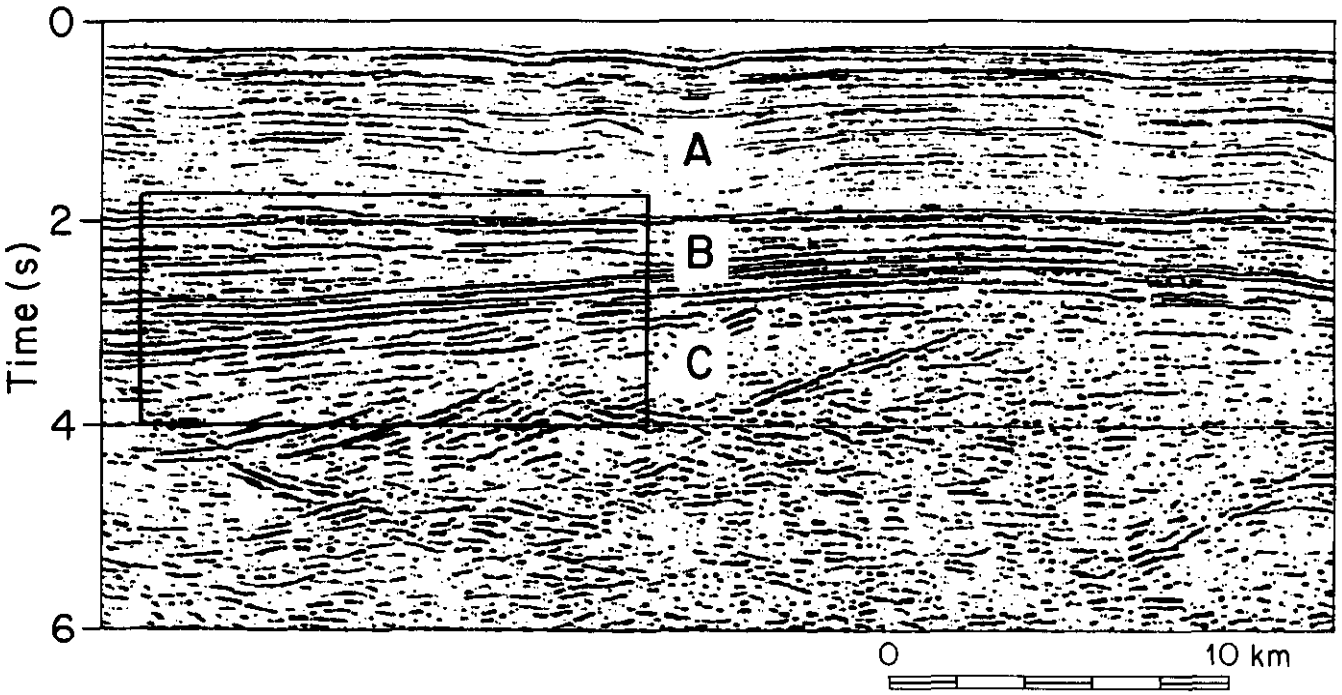

Fig. 4. Marine data example from the Midcontinent Rift (Lake Superior). The migrated section shows highly variable reflector dips and data quality. Multiattribute analysis of a 14-km portion of the data (insert) is shown in Figure 5.

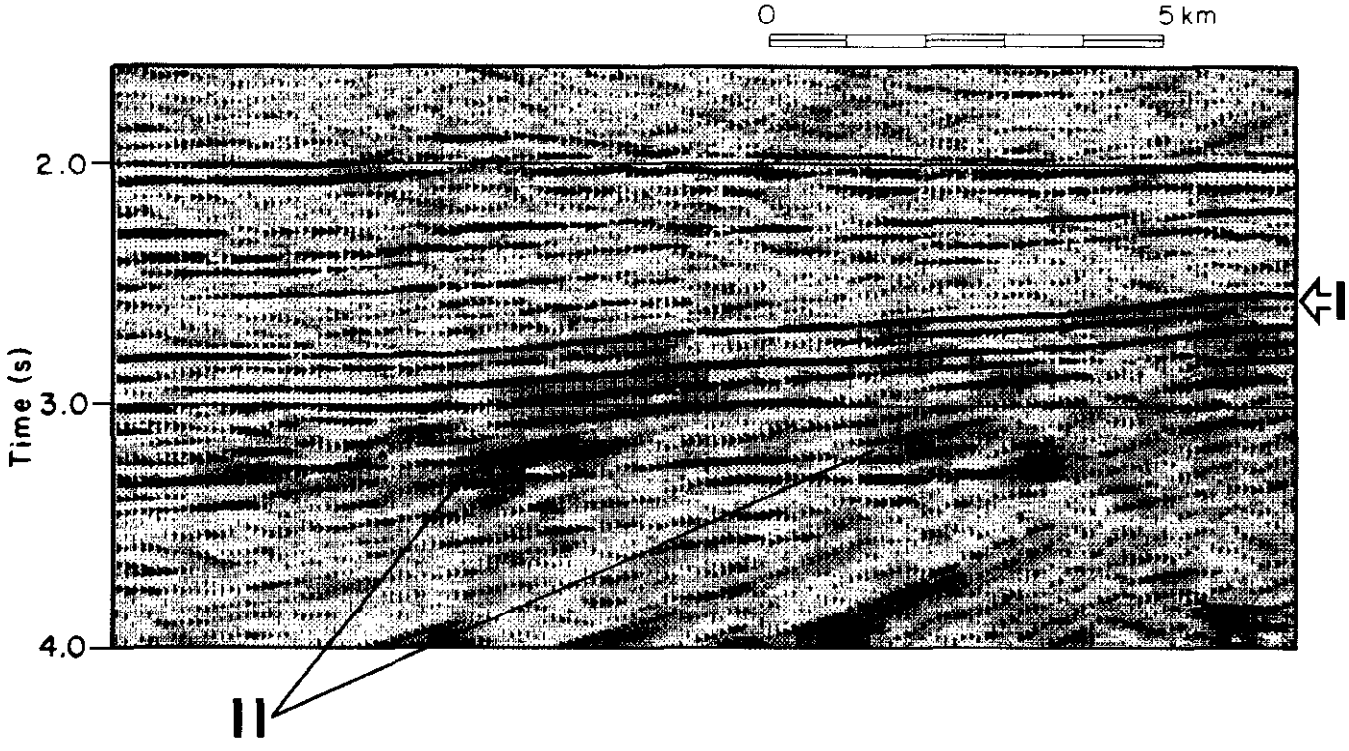

Fig. 5. (a) Multiattribute display with profile overlay. The colour-coded image is based on three attributes: reflection strength, dip estimates and coherency estimates. Note the automatically tracked dip variations associated with the gently dipping reflector (labelled I), the steeply dipping, complex layered reflections underneath (labelled II), between 3 and 3.3 s, and reduced coherency of the data above 2.2 s and below 3.5 s.

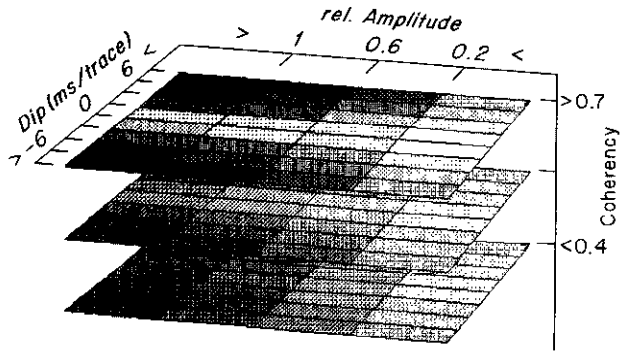

Fig. 5. (b) The colour ring (hue) represents automatically picked dip directions; lightness varies inversely with the 2-D smoothed local estimates of reflection strength, and saturation is controlled by local coherency estimates.

previous section to produce a composite image. Before display, a two-dimensional median filter was applied to the local estimates of reflection strength. Figure 5a shows a subset of this same data presented as a multiattribute image with a data overlay. Attributes are ordered hierarchically in order of their importance, i.e., dip, amplitude and coherency. The three-attribute colour scale is shown in Figure 5b. Dip is represented as hues of 140 to 220 from a scale of 0 to 360, covering apparent dips between +8 and –8 ms/trace. Local reflection strength is represented as lightness with darker shading corresponding to larger amplitudes. The range of amplitudes covered by the lightness scale was carefully adjusted to emphasize the features of most interest. Finally, the saturation of the image was chosen on the basis of local peak semblance estimates. This last step has very little effect on high quality, high semblance parts of the section. However, regions of low data quality appear grey in the HLS scheme display.

The multiattribute display clearly shows the lateral dip variations associated with the base of the volcanic sequence (between 2.5 and 3.0 s, labelled I in Figure 5a). Underneath the layered volcanics (3.0 and 3.3 s) a number of steeply dipping reflections with dips ≥6 ms/trace are highlighted (labelled II). These reflections are believed to be associated with deposition during the early stage of rifting. Also, note the generally reduced coherency of the data above 2.2 s and below 3.5 s.

Discussion and Conclusion

We have implemented a new work station-based seismic display package with the capability of:

a) displaying any of the single-trace or multitrace attributes shown in Figure 1;
b) displaying up to three of these attributes using various colour mixing schemes with or without image processing;
c) interactively manipulating the colour palette to simulate different data cutoffs, scaling and filtering.

These techniques are especially suited for the interpretation of seismic data where lateral variations of attributes are used as indicators of structural changes. The methods described here may also aid in using seismic attributes for the classification and evaluation of lithology (e.g., Huang and Fu, 1987; Lange and Almoghrabi, 1988).

We conclude that HLS mixing schemes are most suitable for problems requiring the display of two or three attributes, especially problems where one quantity is of prime importance to the interpreter.

We now routinely build two-dimensional composite images based on combinations of amplitude, dip and coherency information to assist in the interpretation of seismic data. The method can easily be extended to automatically scan and analyze three-dimensional data volumes.

References

Balch, A.H., 1971, Color sonagrams: a new dimension in seismic data interpretation: Geophysics **36**, 1074-1098.

Bording, R.P., Gersztenkorn, A., Lines, L.R., Scales, J.A. and Treitel, S., 1987, Applications of seismic travel-time tomography: Geophys. J. Roy. Astr. Soc. **90**, 285-303.

Broome, J., 1989, Processing and interpretation of regional geophysical data from the Amer Lake/Wager Bay area, District of Keewatin: M.Sc. thesis, Carleton University.

Cannon, W.F., Green, A.G., Hutchinson, D.R., Lee, M., Milkereit, B., Behrendt, J.C., Halls, H.C., Green, J.C., Dickas, A.B., Morey, G.M., Sutcliffe, R. and Spencer, C., 1989, The North American Midcontinent Rift beneath Lake Superior from GLIMPCE seismic reflection profiling: Tectonics **8**, 305-332.

Cliet, C. and Dubesset, M., 1987, Three-component recordings: interest for land seismic source study: Geophysics **52**, 1048-1059.

Dalley, R.M., Gevers, E.C.A., Stampfli, G.M., Davies, D.J., Gastaldi, C.N., Ruitjenberg, P.A. and Vermeer, G.J.O., 1989, Dip and azimuth displays for 3D seismic interpretation: First Break **7**, 86-95.

Duval, J.S., 1983, Composite color images of aerial gamma-ray spectrometric data: Geophysics **48**, 722-735.

Fraiser, C. and Winterstein, K., 1990, Analysis of conventional and converted mode reflections at Putah sink, California using three-component data: Geophysics **55**, 646-659.

Gersztenkorn, A. and Scales, J.A., 1988, Smoothing seismic tomograms with alpha-trimmed means: Geophys. J. **92**, 67-72.

Hardy, R.J.J., Warner, M.R. and Hobbs, R.W., 1989, Labeling long-period multiple reflections: Geophysics **54**, 122-126.

Horn, B.K.P., 1982, Hill shading and the reflectance map: Geo-Processing **2**, 65-146.

Huang, K.Y. and Fu, K.S., 1987, Detection of seismic bright spots using pattern recognition techniques, *in* Aminzadeh, F., Ed., Pattern recognition & image processing: handbook of seismic exploration: Vol. 20, Geophysical Press, 263-301.

_____, Yang, G.J. and Tang, G.Y., 1979, A fast two-dimensional median filtering algorithm: Inst. Electr. Electron. Eng., Trans. **ASSP-27**, 13-18.

Lange, J.N. and Almoghrabi, H.A., 1988, Lithology discrimination for thin layers using wavelet signal parameters: Geophysics **53**, 1512-1519.

Leven, J.H. and Roy-Chowdhury, K., 1984, A semblance-weighted slowness filter in the time domain: 54th Ann. Internat. Mtg., Soc. Expl. Geophys., Expanded Abstracts, 432-436.

Lindseth, R.O., 1979, Synthetic sonic logs – a process for stratigraphic interpretation: Geophysics **44**, 3-26.

McMechan, G.A., 1983, P-x imaging by localized slant stack of t-x data: Geophys. J. Roy. Astr. Soc. **72**, 213-221.

Milkereit, B., 1987a, Migration of noisy crustal seismic data: J. Geophys. Res. **92**, 7916-7930.

_____, 1987b, Decomposition and inversion of seismic data — an instantaneous slowness approach: Geophys. Prosp. **35**, 875-894.

_____ and Spencer, C., 1990, Noise suppression and coherency enhancement of seismic data, *in* Agterberg, F. and Bonham-Carter, G., Eds., Statistical applications in the earth sciences: GSC paper 89-9, 243-248.

Oldenburg, D.W., Sheuer, T. and Levy, S., 1983, Recovery of the acoustic impedance from reflection seismograms: Geophysics **48**, 1318-1337.

Quincy, E.A. and Tomich, D.J., 1987, Image processing of seismograms using two-dimensional coherency techniques, *in* Aminzadeh, F., Ed., Pattern recognition & image processing: handbook of seismic exploration: Vol. 20, Geophysical Press, 110-156.

Rots, A.H., 1989, Special purpose image display devices and techniques at the National Radio Astronomy Observatory: Computers in Physics, Nov/Dec, 41-46.

Stewart, R.R., 1985, Median filtering: review and new f/k analogue design: J. Can. Soc. Expl. Geophys. **21**, 54-63.

Taner, M.T. and Sheriff, R.E., 1977, Application of amplitude, frequency and other attributes to stratigraphic and hydrocarbon determination, *in* Payton, C.E., Ed., Seismic stratigraphy — applications to hydrocarbon exploration: Am. Assn. Petr. Geol., Mem. 26, 301-327.

_____ , Koehler, F. and Sheriff, R.E., 1979, Complex trace analysis: Geophysics **44**, 1041-1063.

Varsek, J.L., Cook, F.A. and Cheadle, S.P., 1990, Enhanced crustal reflection continuity by estimation of statics from coherency filtered sections: Geophys. Res. Lett. **17**, 231-234.

Watson, K., 1985, Remote sensing — a geophysical perspective: Geophysics **50**, 2595-2610.